



## Original Article

# Hypertonic Saline and Aprotinin Inhibit Furin and Nasal Protease to Reduce SARS-CoV-2 Specific Furin Site Cleavage Activity



Clarissa Li and Adam W. Li\*

EpigenTek Group Inc., New York, USA

Received: December 06, 2021 | Revised: June 10, 2022 | Accepted: June 23, 2022 | Published: August 03, 2022

## Abstract

**Background and objectives:** Severe acute respiratory syndrome coronavirus 2 (SARS-CoV-2) enters the human body mainly through the nasal epithelial cells. The cell entry of SARS-CoV-2 needs to be preactivated via S1/S2 boundary furin motif cleavage by furin and/or relevant proteases. Therefore, it is important to locally block the SARS-CoV-2 S1/S2 site cleavage caused by furin and other relevant protease activity in the nasal cavity.

**Methods:** With synthesized peptides containing a wild-type or mutant furin cleavage motif and by using SARS-CoV-2 specific furin site cleavage assay, we tested the hypertonic saline and aprotinin-based blockage of the SARS-CoV-2 specific furin site cleavage by furin, trypsin, and nasal swab samples containing nasal proteases.

**Results:** The results showed that hypertonic saline and aprotinin could block SARS-CoV-2 specific furin site cleavage, and a hypertonic saline and aprotinin combination could reduce 99% of the furin site cleavage in the SARS-CoV-2 wild-type, 90% in the P681R mutant, and 83% in the N679K/P681H mutants, respectively by inhibition of the nasal protease activity.

**Conclusions:** Our findings preliminarily elucidated that the combination of hypertonic saline and aprotinin significantly blocked the furin site cleavage in both the SARS-CoV-2 wild-type and mutants (P681R and N679K/P681H), which could represent a simple, economical, and practical feasible approach in locally controlling viral activation and entry into cells to replicate.

## Introduction

The recent coronavirus disease 2019 (COVID-19) pandemic was

caused by severe acute respiratory syndrome coronavirus 2 (SARS-CoV-2), a new member of the same coronavirus family that caused SARS and Middle East respiratory syndrome. To date, more than 530 million infections and 6.3 million deaths have been reported worldwide,<sup>1</sup> and the numbers continue to rise because of the increased COVID-19 variants, such as the Delta and Omicron strains that have resulted from viral mutations. There are also no effective drugs that could be currently used for the prevention and treatment of COVID-19. Nevertheless, the vaccines against COVID-19 have achieved excellent effects on preventing and reducing the original SARS-CoV2 infections. However, the vaccine effects have been significantly reduced against the COVID-19 variants, such as Omicron that is currently the dominant variant in the USA and many other countries.<sup>2,3</sup>

It was found that the SARS-CoV-2 spike (S) glycoprotein harbors a furin cleavage site (FCS) at the boundary between the S<sub>1</sub>/S<sub>2</sub> subunits, which could be cleaved by furin and/or the relevant

**Keywords:** SARS-CoV-2; Furin cleavage site; Nasal protease; Hypertonic saline; Aprotinin; Mutant.

**Abbreviations:** ENaC, epithelial sodium channel; FCS, furin cleavage site; HAT, human airway trypsin; KLK1, kallikrein 1; NaCl, sodium chloride; PBS, phosphate buffered saline; PBS-T, phosphate buffered saline-tween 20; PC, protease cleavage; RT, room temperature; TMB, 3,3',5,5'-tetramethylbenzidine.

\***Correspondence to:** Adam W. Li, EpigenTek Group Inc., 110 Bi County Boulevard, Suite 122, Farmingdale, New York 11735, USA. ORCID: <https://orcid.org/0000-0001-8231-8175>. Tel: +01-718-484-3990, Fax: +01-631 815-6729, E-mail: [awli@epigentek.com](mailto:awli@epigentek.com)

**How to cite this article:** Li C, Li AW. Hypertonic Saline and Aprotinin Inhibit Furin and Nasal Protease to Reduce SARS-CoV-2 Specific Furin Site Cleavage Activity. *J Explor Res Pharmacol* 2022;00(00):00-00. doi: 10.14218/JERP.2021.00058.

proteases secreted from the host cells. Unlike SARS-CoV, the cell entry of SARS-CoV-2 needs to be preactivated by furin and/or the relevant proteases, thus reducing its dependence on target cell proteases for entry. The activation of the S-protein through two sequential proteolytic cleavage steps has well demonstrated to be essential for the SARS-CoV-2 spike-mediated virus binding to the host ACE2 receptor, cell-cell fusion, and viral entry into human lung cells.<sup>4,5</sup> It was also observed that other viruses containing a FCS, such as H5N1, displayed increased replicates and developed higher pathogenicity.<sup>6</sup>

The complete SARS-CoV-2 FCS was characterized as a 20 amino acid motif that corresponded to the amino acid sequence A672-S691 of the SARS-CoV-2 spike protein (QOS45029.1) with one core region SPRRAR|SV (eight amino acids; S680-V687) and two flanking solvent accessible regions (eight amino acids; A672-N679, and four amino acids; A688-S691). The core region was very unique as its R683 and A684 positions were positively charged (Arg), and it had hydrophobic (Ala) residues, respectively, which allowed this site to not only be cleaved by serine protease furin or furin-like PCs, but also permitted the cleavage efficiency to be facilitated by other serine proteases targeting mono- and dibasic amino acid sites, such as matriptase, kallikrein 1 (KLK1), human airway trypsin (HAT), and TMPRSS2. Furthermore, mutation of P681 (non-polar proline) to become positive R681 to form multibasic amino acid sites in the Delta variant could increase the S1/S2 boundary cleavage, thereby increasing the viral replicates in the human airways and transmission.<sup>7,8</sup> In addition, double mutation of N679K and P681H, which formed more basic amino acid sites in the FCS, shared by all Omicron variants including BA.2 and BA.2.12.1, has made the Omicron variants to be extremely transmissible.<sup>9</sup>

It was demonstrated that SARS-CoV-2 enters the human body mainly through the nasal epithelial cells.<sup>10</sup> There are high levels of furin and other facilitating serine proteases, which are secreted from the nasal epithelial cells and generated from bacteria in the nasal cavity. Thus, it would be important to locally block the SARS-CoV-2 S1/S2 site cleavage caused by furin and other facilitating serine protease activity in the nasal cavity as the furin-based SARS-CoV-2 S1/S2 cleavage would increase the SARS-CoV-2 entry into the cells resulting in its replication, and eventually developing higher pathogenicity and transmission of COVID-19. It was reported that hypertonic saline (1.2–3%) could significantly inhibit the urinary protease-mediated cleavage of the epithelial sodium channel (ENaC) substrate containing the RRAR furin site.<sup>11</sup> Aprotinin is a broad serine protease inhibitor against various serine proteases. We thus tested the hypertonic saline and aprotinin-based blockage of the SARS-CoV-2-specific FCS by furin and other facilitating serine proteases. The results showed that hypertonic saline and aprotinin blocked the SARS-CoV-2 specific FCS and that a hypertonic saline and aprotinin combination could significantly reduce the SARS-CoV-2 wild-type and mutant FCS by inhibition of the nasal protease activity.

## Methods

### *Synthesis of peptide containing the SARS-CoV-2 specific furin cleavage site*

The dual-tagged peptides containing the wild-type, mutant P681R, mutants N679K/P681H and triple R-deleted SARS-CoV-2-specific furin motif were synthesized through a Biomatik platform of peptide synthesis services. The peptide was labeled with polyhistidine at the N terminal and biotin at the C terminal.

### *Sample collection*

Collection of the nasal swab samples from healthy uninfected volunteers was in accordance with the standard Centers for Disease Control and Prevention (CDC) nasal swab collection protocol. The procedure involved human samples that were exempt from the institutional review board (IRB)'s review and approval, as this study fitted into a defined exempt category of the IRB's general criteria (Supplementary File 1). The collected samples were released into 300 µl of protease cleavage (PC) assay buffer (EpiGentek) or a sodium chloride (NaCl) solution at different concentrations by rotating the swab in the buffer for 30 sec. The solution was centrifuged at 12,000 rpm at room temperature (RT) for 1 min. The supernatant was collected and freshly used for the assay.

### *Measurement of the SARS-CoV-2 specific furin site cleavage*

The FCS measurement was carried out as described.<sup>12</sup> In brief, the synthesized peptides containing the wild-type, mutant P681R, mutants N679K/P681H and triple R-deleted SARS-CoV-2-specific furin motif were diluted with phosphate buffered saline (PBS) and added at a concentration of 5 ng/well to the Ni-NTA-coated strips and incubated for 1 h at RT. After washing the strips three times with phosphate buffered saline-tween 20 (PBS-T), purified furin (New England Biolabs) and protease trypsin (Sigma) were added at different concentrations and incubated for 25 min at a temperature of 37°C. The PC assay buffer (EpiGentek) was used as the assay solutions. After washing for four times, streptavidin-HRP (1:5,000 dilution) was added and incubated for 30 min at RT. After washing for four times again, 100 µl of 3,3',5,5'-tetramethylbenzidine (TMB) solution was added per well and the development of the blue color was monitored for 2–10 min. The reaction was stopped with hydrochloric acid (HCl), and the optical density was measured with a microplate reader at a wavelength of 450 nm.

### *Hypertonic saline and aprotinin blockage of the furin- and trypsin-mediated furin cleavage site*

His- and biotin-tagged peptides containing the wild-type and mutant SARS-CoV-2-specific furin motif were added at a concentration of 5 ng/well to the Ni-NTA-coated wells of the 8-well microplate strips and incubated for 1 h at RT. Simultaneously, the furin or trypsin diluted in the PC solution was incubated with hypertonic saline or aprotinin at different concentrations for 10 min. After washing the strips for three times with PBS-T, the enzyme solutions pre-incubated with NaCl (Sigma) or aprotinin (Sigma) at different concentrations were transferred into the strip wells and incubated for 25 min at a temperature of 37°C. After washing for four times, streptavidin-HRP (1:5,000 dilution) was added and incubated for 30 min at RT. After washing for four times again, 100 µl of TMB solution were added per well, and development of the blue color was monitored for 2–10 min. The reaction was stopped with HCl, and the optical density was measured with a microplate reader at a wavelength of 450 nm.

### *Hypertonic saline and aprotinin based inhibition of the nasal protease-mediated furin cleavage site*

His- and biotin-tagged peptides containing the wild-type and mutant SARS-CoV-2-specific furin motif were added at a concentra-

**Table 1.** The list and sequence of the SARS-CoV-2 wild-type and mutant FCS peptides

Peptide	Sequence
Wild-type	ASYQTQTNSPRRRARSVASQS
P681R	ASYQTQTNSRRRARSVASQS
N679K/P681H	ASYQTQTKSHRRARSVASQS
Triple-R-deletion	ASYQTQTNSPASVASQS

tion of 5 ng/well to the Ni-NTA-coated wells of the 8-well microplate strips and incubated for 1 h at RT. After washing the strips for three times with PBS-T, the nasal swab sample supernatant was incubated with hypertonic saline (3%), or aprotinin (2 µg/well), or hypertonic saline combined with aprotinin for 10 min. The sample solutions were then transferred into the strip wells and incubated for 25 min at a temperature of 37°C. After washing for four times, streptavidin-HRP (1:5,000 dilution) was added and incubated for 30 min at RT. After washing for four times again, 100 µl of TMB solution were added per well and development of the blue color was monitored for 2–10 min. The reaction was stopped with HCl, and the optical density was measured with a microplate reader at a wavelength of 450 nm.

### Statistical analysis

The data were presented as the mean ± standard deviation (SD). The cleavage percentage of the enzyme-treated samples incubated with or without hypertonic saline and aprotinin was calculated as follows:

$$\text{Cleavage \%} = \left( 1 - \frac{\text{OD treated} - \text{OD blank}}{\text{OD untreated control} - \text{OD blank}} \right) \times 100\%$$

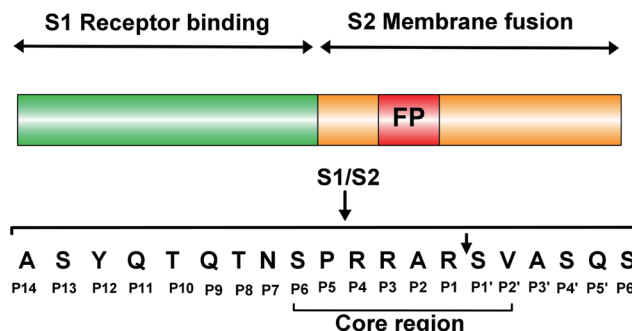
A two-tailed *t*-test was used for the analysis of the differences between the mean of each group.

## Results

### Cleavage of both the wild-type and mutant furin cleavage site by furin and trypsin

The sequences of the synthesized peptides (Table 1) were based on the complete SARS-CoV-2 FCS characterized as a 20 amino acid motif (Fig. 1). The experimental procedure is shown in Figure 2.

The dual-tagged peptides with polyhistidine at the N-terminal and biotin at the C-terminal were bound onto microplate wells through histidine/Ni-NTA at its N-terminal. The cleavage of the peptides in the FCS core region removed the C-terminal part of the peptides after washing, which caused a decrease in the signal generated by the avidin/biotin binding after adding streptavidin-HRP. As shown in Figure 3a and b, the furin enzyme cleaved the wild-type, P681R and N679K/P681H mutant FCS, but not the triple R-deleted FCS in a concentration dependent manner. Serine protease trypsin could cleave the wild-type, P618R and N679K/P681H FCS with a higher cleavage percentage even at 10 ng of the concentration. However, the triple R-deleted FCS peptide was also not cleaved by trypsin. These results were consistent with our previously reported data.<sup>12</sup> We would thus focus on the wild-type, P681R, and N679K/P681H mutant types in future studies.

**Fig. 1.** Schematic of the SARS-CoV-2 spike protein, and the furin cleavage site at the boundary between the S1 and S2 subunits.

### Cleavage of both the wild-type and mutant furin cleavage site by the nasal swab sample

We also tested the FCS cleavage of these peptides by nasal swab samples. Endogenous proteases from the nasal mucosa and exogenous proteases from the bacterial flora of the nasal cavity could be captured by a nasal swab. As shown in Figure 4, both the wild-type and mutant (P681R and N679K/P681H) FCS peptides were cleaved by a nasal swab solution in a concentration-dependent manner. At a 25 µl solution volume that was only 10% of the collected sample supernatant volume, 70–80% of the wild type and mutant FCS peptides were cleaved, and the cleavage level was not significantly different among the wild-type, P681R, and N679K/P681H mutants ( $p > 0.05$ ).

### Hypertonic saline and aprotinin block the furin- and trypsin-induced cleavage of both the wild-type and mutant furin cleavage site

We further examined the effects of hypertonic saline and aprotinin on the FCS blockage of these peptides. Dual His- and biotin-tagged FCS peptides were bound to the Ni-coated microplate wells. The wells were then exposed to the furin or trypsin solution, which was pre-incubated with hypertonic saline or aprotinin at different concentrations. As shown in Figure 5a, normal saline (0.9%) did not show the inhibitory effect on the furin enzyme-caused cleavage of the FCS peptides. Higher saline concentrations (1.5%) effectively blocked the cleavage of both the wild-type and mutant FCS caused by the furin enzyme. At 3% of the salt concentration, around 80% of the furin cleavage had an effect on the wild-type, 70% of the P681R mutant, and 61% of the N679K/P681H mutants, which were significantly inhibited ( $p < 0.05$ ), respectively. In contrast, the trypsin-caused cleavage of the wild-type and mutant FCS was only slightly inhibited (<30%) by hypertonic saline even at concentrations of 3% (Fig. 5b). The aprotinin exhibited a dose-dependent inhibition of the furin- and trypsin-induced cleavage of the wild-type and mutant FCS (Fig. 5d). At 2 µg per well (around 6 µM), aprotinin decreased 65–82% of the furin cleavage ( $p < 0.05$ ) and 85–97% of the trypsin cleavage ( $p < 0.01$ ), respectively.

### Hypertonic saline and aprotinin block the nasal swab sample-caused cleavage of both the wild-type and mutant furin cleavage site by inhibition of the nasal protease activity.

The inhibition of the nasal swab sample-caused cleavage of the

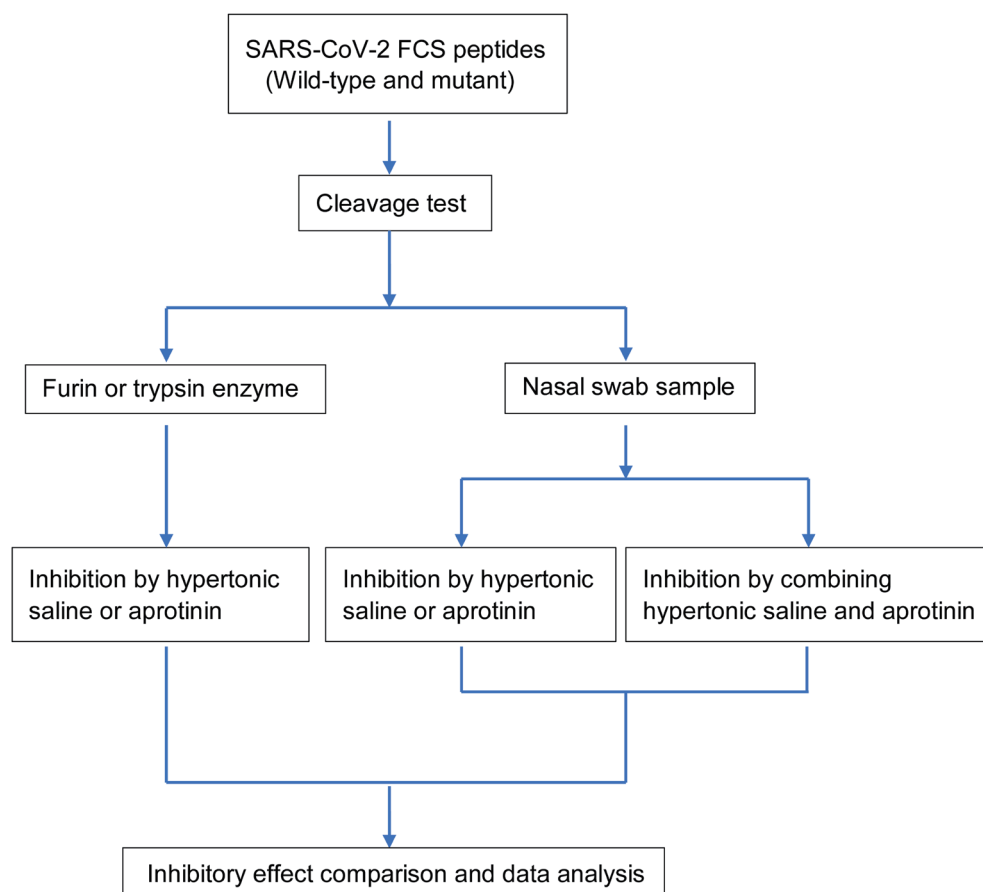


Fig. 2. Flow chart of the experimental procedure for the cleavage assay and inhibition of the SARS-CoV-2 specific FCS.

peptide FCS by hypertonic saline and aprotinin was next examined. As shown in Figure 6, in the wild-type, the cleavage was reduced from 60.7% to 22% by hypertonic saline (3%) and from 60.7% to 41.5% by 2  $\mu$ g of aprotinin. In the P681R mutant type, the cleavage was only decreased to 51.7% from 69.5% by hypertonic saline and to 63.5% from 69.5% by aprotinin. In contrast, in the N679K/P681H mutants, the cleavage was decreased

to 19% from 68% by hypertonic saline and to 31.25% from 68% by aprotinin. However, the decreased cleavage was significant when combining the hypertonic saline and aprotinin. Nasal swab sample-caused cleavage was reduced to 0.5% from 60.7% in the wild-type ( $p < 0.01$ ), to 10% from 69.5% in the P681R mutant ( $p < 0.05$ ), and to 8.8% from 68% in the N679K/P681H mutants ( $p < 0.01$ ), respectively.

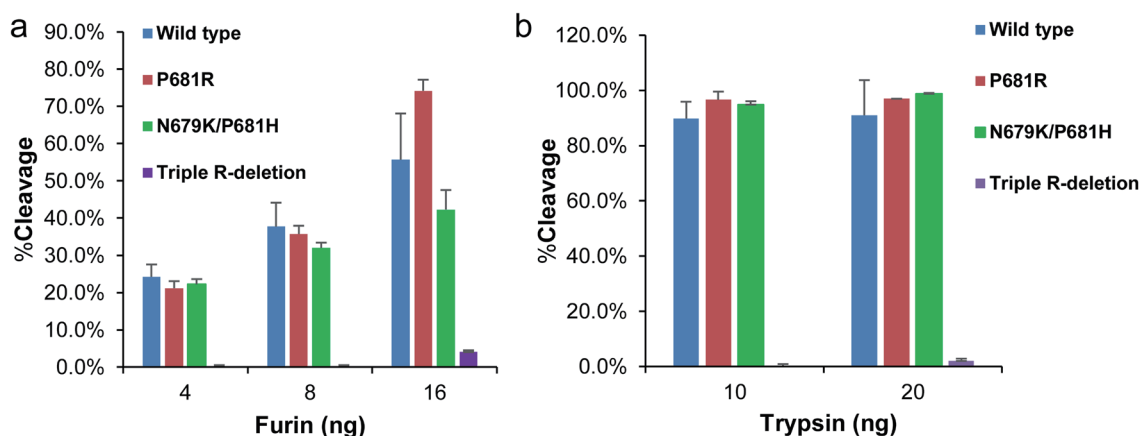


Fig. 3. Cleavage of the SARS-CoV-2 wild-type, P681R, N679K/P681H and triple R-deletion mutant FCS by the serine proteases at different concentrations. a). furin; b). trypsin. No significant difference of the cleavage level ( $p > 0.05$ ) caused by furin or trypsin among the wild-type, P681R, and N679K/P681H mutants.

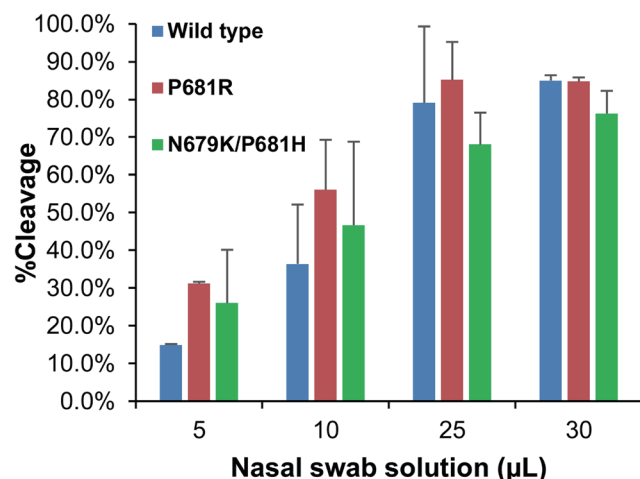


Fig. 4. Cleavage of the SARS-CoV-2 wild-type, P681R, and N679K/P681H mutant FCS by the nasal swab sample at different amounts. NO significant difference of the cleavage level ( $p > 0.05$ ) caused by the nasal swab sample among the wild-type, P681R, and N679K/P681H mutants.

## Discussion

In this study, we utilized the synthesized peptides containing the

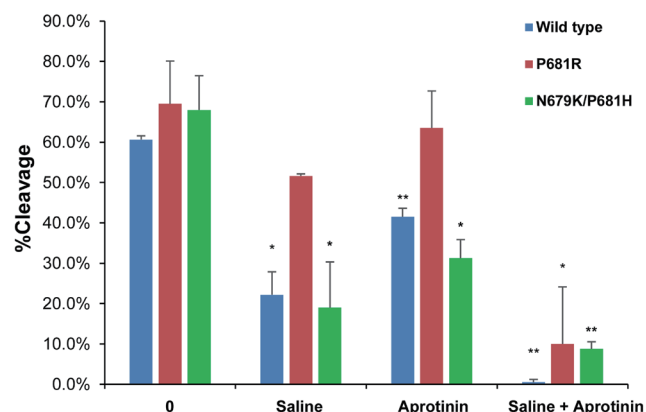


Fig. 6. Blockage of the SARS-CoV-2 wild-type P681R, and N679K/P681H mutant FCS caused by the nasal swab samples. Hypertonic saline alone: 3%; aprotinin alone: 2 µg/well; hypertonic saline and aprotinin combination: 3% + 2 µg. \* $p < 0.05$ ; \*\* $p < 0.01$ .

wild-type or mutant FCS to examine the effect of hypertonic saline and serine proteinase inhibitor aprotinin on the blockage of the SARS-CoV-2 specific FCS. Our previous study showed both the SARS-CoV-2 S protein, and the synthesized wild-type FCS peptide could be bound and immunocaptured by the SARS-CoV-2-specific furin site blocking the antibody in a concentration-de-

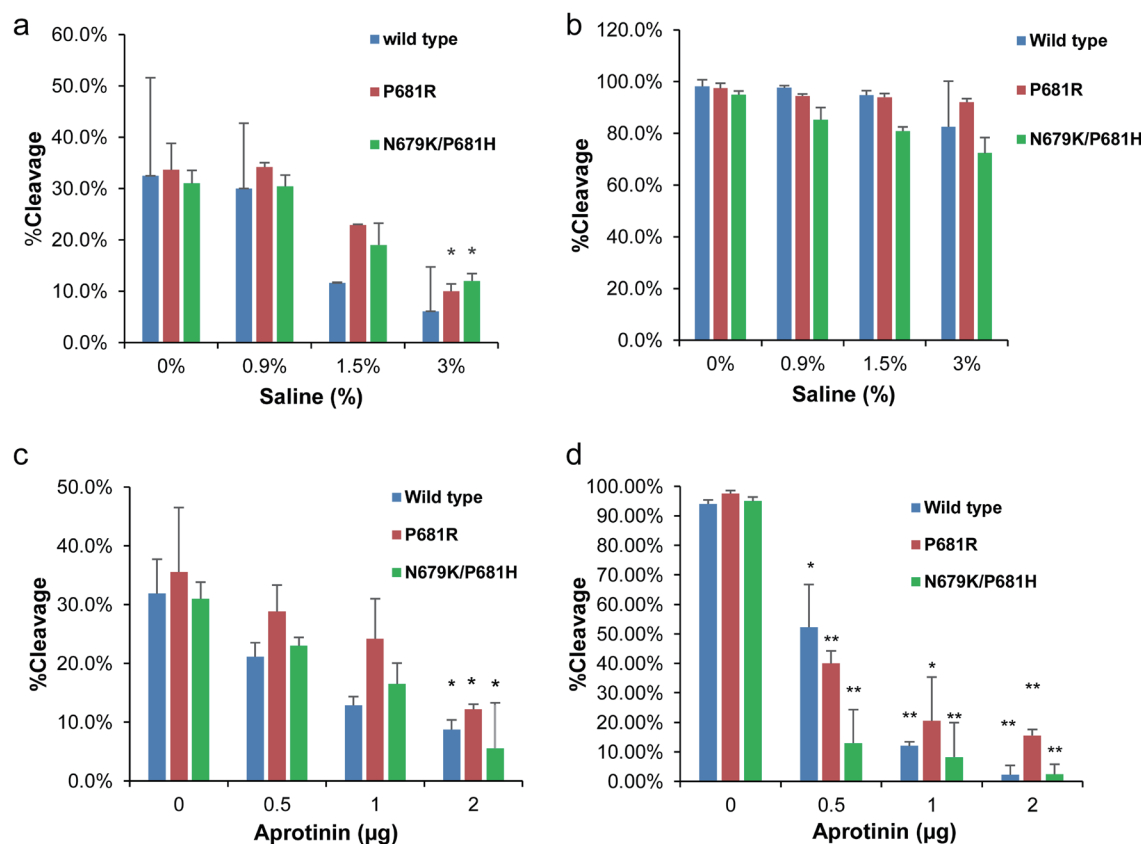


Fig. 5. Blockage of the SARS-CoV-2 wild-type, P681R, and N679K/P681H mutant FCS cleavage caused by furin and trypsin. A) Hypertonic saline blockage on the furin (8 ng/well) cleavage. B) Hypertonic saline blockage on the trypsin (10 ng/well) cleavage. C) Aprotinin blockage on the furin (8 ng/well) cleavage. D) Aprotinin blockage on the trypsin (10 ng/well) cleavage. \* $p < 0.05$ ; \*\* $p < 0.01$ .



pendent manner.<sup>12</sup> Furthermore, both the synthesized peptide and full-length S-protein were cleaved to a similar level by the recombinant furin protein. As a consequence, the results indicated that the synthesized peptide was the same as the biological S protein as a SARS-CoV-2-specific FCS cleavage assay substrate.

In addition, it was demonstrated that the hypertonic saline resulted in a dose-dependent inhibition of the replication of a range of DNA and RNA viruses, including the human coronavirus 229E (HCoV-229E).<sup>13</sup> Hypertonic saline nasal irrigation and gargling was also found to reduce viral upper respiratory tract infection in a clinical trial.<sup>14,15</sup> Recently, hypertonic saline (1.5% NaCl) was shown to significantly inhibit the replication of SARS-CoV-2 in cultured human lung and kidney epithelial cells. The major mechanism was possibly through sodium ion-mediated intracellular low energy states.<sup>16</sup> In this study, we observed that in both the wild-type and mutants, hypertonic saline could significantly block the SARS-CoV-2-specific FCS cleavage caused by furin but not by trypsin. As S protein cleavage played a critical role in the SARS-CoV-2 activation before entry into and exiting from the cells, the inhibitory effect of hypertonic saline on the SARS-CoV-2 replication could be at least partly due to the blockage of the furin-mediated cleavage. Aprotinin was approved by the Food and Drug Administration for clinical use for reducing bleeding during complex surgery.<sup>17</sup> However, it showed significant antiviral effects against H1N1 influenza infections both *in vitro* and *in vivo* by blocking HA cleavage and activation.<sup>18</sup> Bojkova *et al.* recently reported that aprotinin was able to inhibit SARS-CoV-2 replication to block a SARS-CoV-2-induced cytopathogenic effect formation at therapeutically achievable concentrations.<sup>19</sup> Our study showed that the aprotinin effect at the 3–6  $\mu$ M level was remarkable in decreasing the trypsin-mediated SARS-CoV-2 FCS cleavage but only moderate in inhibiting the furin-based FCS cleavage.

We observed that higher cleavage percentages were achieved with furin for the P681R FCS peptide than for the wild-type one. This was consistent with the Delta variant's P681R that allowed the cleavage to occur more easily than in the wild-type SARS-CoV-2 strain, as the Delta variant had a more efficient furin cleavage site.<sup>20,21</sup> Nonetheless, the cleavage level with furin for the N679K/P681H FCS peptide was similar to that for the wild-type one, which was consistent with that of the two mutations (N679K/P681H) in Omicron near the FCS that may not enhance the S protein cleavage.<sup>22</sup> Yet, the cleavage of the mutant FCS by furin could still be inhibited by hypertonic saline or aprotinin at an appropriate concentration even if such inhibition was relatively less in the mutant FCS compared to the wild-type. An interesting observation in this study was that significant cleavage in both the wild-type and mutant FCS peptide could be obtained by trypsin, which suggested the important role of facilitating the serine proteases in both the wild-type and mutant SARS-CoV-2 FCS. We also observed that the combination of hypertonic saline and aprotinin achieved nearly complete inhibition of the FCS in both the wild-type and mutants with use of nasal swab samples although hypertonic saline or aprotinin alone only had a moderate and mild inhibitory effect on both the wild-type and mutants, respectively. This additive effect would suggest the importance of the combination of hypertonic saline and aprotinin in practical use for SARS-CoV-2-specific FCS inhibition, as the nasal proteases could be from both the host cells and bacteria in the nasal cavity. Hence, these proteases relevant to the FCS could include both furin/furin-like proprotein convertases targeting the furin cleavage motif and trypsin/trypsin-like serine proteases targeting mono or multiple arginine in FCS, which could be from different sensitivity to hypertonic saline and aprotinin.

Furthermore, it has been generally accepted that the nasal epithelium is the initial source of the SARS-CoV-2 infection and proliferation,<sup>23,24</sup> where nasal protease-mediated S protein cleavage causes

viral activation and replication.<sup>25</sup> In the absence of effective drugs and decrease in the vaccine effect against the Delta and Omicron variants, topical application of hypertonic saline combined with aprotinin, such as nasal drops or aerosol could represent a simple, economical, practical feasible approach, which would be greatly helpful in locally controlling viral activation and entry into cells to replicate, thereby reducing and preventing SARS-CoV-2 infection and avoiding the progress of COVID-19 to be a severe and systemic disease.

### Future directions

We plan to carry out more experiments to examine the inhibitory effects of the experimental condition on virus entry and replication in sensitive cells. We would also evaluate the *in vivo* effect of the combination of hypertonic saline and aprotinin. Future experiments would help to see if hypertonic saline and aprotinin-based local control of viral activation and entry into the cells to replicate could be achieved at the *in vivo* level.

### Conclusions

Our findings preliminarily elucidated that the combination of hypertonic saline and aprotinin significantly blocked the FCS in both the SARS-CoV-2 wild-type and mutants (P681R and N679K/P681H), which could represent a simple, economical, and practically feasible approach in locally controlling viral activation and entry into cells to replicate.

### Supporting information

Supplementary material for this article is available at <https://doi.org/10.14218/JERP.2021.00058>.

### Supplementary File 1. STROBE Checklist.

### Acknowledgments

None.

### Funding

This work was supported by research and development funding from the EpigenTek Group Inc. No grants were received from other sources in support of this research work.

### Conflict of interest

Adam W. Li is the scientific founder and CSO of EpiGentek, who has stock and/or stock options in the company, and Clarissa Li is the technician of EpiGentek.

### Author contributions

Contribution to the study's concept and design (CL and AWL),

experiment performance (CL and AWL), data analysis (AWL), drafting of the manuscript (CL and AWL), critical revision of the manuscript (AWL), and supervision (AWL).

## Ethical statement

The procedure involving human samples was exempt from the IRB's review and approval, as this study fitted into a defined exempt category of the IRB's general criteria.

## Data sharing statement

No additional data are available.

## References

- [1] Coronavirus Cases-Worldometer (Updated May 20, 2022). Available from: <https://www.worldometers.info/coronavirus/>. Accessed June 10, 2022.
- [2] Menni C, Valdes AM, Polidori L, Antonelli M, Penamakuri S, Nogal A, *et al*. Symptom prevalence, duration, and risk of hospital admission in individuals infected with SARS-CoV-2 during periods of omicron and delta variant dominance: a prospective observational study from the ZOE COVID Study. *Lancet* 2022;399(10335):1618–1624. doi:10.1016/S0140-6736(22)00327-0, PMID:35397851.
- [3] Statement on Omicron sublineage BA.2. Available from <https://www.who.int/news/item/22-02-2022-statement-on-omicron-sublineage-ba.2>. Accessed June 10, 2022.
- [4] Hoffmann M, Kleine-Weber H, Pöhlmann S. A Multibasic Cleavage Site in the Spike Protein of SARS-CoV-2 Is Essential for Infection of Human Lung Cells. *Mol Cell* 2020;78(4):779–784.e5. doi:10.1016/j.molcel.2020.04.022, PMID:32362314.
- [5] Hoffmann M, Kleine-Weber H, Schroeder S, Krüger N, Herrler T, Erichsen S, *et al*. SARS-CoV-2 Cell Entry Depends on ACE2 and TMPRSS2 and Is Blocked by a Clinically Proven Protease Inhibitor. *Cell* 2020;181(2):271–280.e8. doi:10.1016/j.cell.2020.02.052, PMID:32142651.
- [6] Decha P, Rungrotmongkol T, Intharathap P, Malaisree M, Aruksakunwong O, Laothongpaysan C, *et al*. Source of high pathogenicity of an avian influenza virus H5N1: why H5 is better cleaved by furin. *Biophys J* 2008;95(1):128–134. doi:10.1529/biophysj.107.127456, PMID:18375507.
- [7] Mlcochova P, Kemp SA, Dhar MS, Papa G, Meng B, Ferreira IATM, *et al*. SARS-CoV-2 B.1.617.2 Delta variant replication and immune evasion. *Nature* 2021;599(7883):114–119. doi:10.1038/s41586-021-03944-y, PMID:34488225.
- [8] Davies NG, Abbott S, Barnard RC, Jarvis CI, Kucharski AJ, Munday JD, *et al*. Estimated transmissibility and impact of SARS-CoV-2 lineage B.1.1.7 in England. *Science* 2021;372(6538):eabg3055. doi:10.1126/science.abg3055, PMID:33658326.
- [9] Kandeel M, Mohamed MEM, Abd El-Lateef HM, Venugopala KN, El-Beltagi HS. Omicron variant genome evolution and phylogenetics. *J Med Virol* 2022;94(4):1627–1632. doi:10.1002/jmv.27515, PMID:34888894.
- [10] Sungnak W, Huang N, Bécavin C, Berg M, Queen R, Litvinukova M, *et al*. SARS-CoV-2 entry factors are highly expressed in nasal epithelial cells together with innate immune genes. *Nat Med* 2020;26(5):681–687. doi:10.1038/s41591-020-0868-6, PMID:32327758.
- [11] Berman JM, Awayda RG, Awayda MS. Effects of urine composition on epithelial Na<sup>+</sup> channel-targeted protease activity. *Physiol Rep* 2015;3(11):e12611. doi:10.14814/phy2.12611, PMID:26564065.
- [12] Spelios MG, Capanelli JM, Li AW. A novel antibody against the furin cleavage site of SARS-CoV-2 spike protein: Effects on proteolytic cleavage and ACE2 binding. *Immunol Lett* 2022;242:1–7. doi:10.1016/j.imlet.2022.01.002, PMID:35007661.
- [13] Ramalingam S, Cai B, Wong J, Twomey M, Chen R, Fu RM, *et al*. Anti-viral innate immune response in non-myeloid cells is augmented by chloride ions via an increase in intracellular hypochlorous acid levels. *Sci Rep* 2018;8(1):13630. doi:10.1038/s41598-018-31936-y, PMID:30206371.
- [14] Ramalingam S, Graham C, Dove J, Morrice L, Sheikh A. A pilot, open labelled, randomised controlled trial of hypertonic saline irrigation and gargling for the common cold. *Sci Rep* 2019;9(1):1015. doi:10.1038/s41598-018-37703-3, PMID:30705369.
- [15] Baxter AL, Scheartz KR, Johnson RW, Rao ASRS, Gibson RW, Cherian E, *et al*. Rapid initiation of nasal saline irrigation: hospitalizations in COVID-19 patients randomized to alkalization or povidone-iodine compared to a national dataset. *MedRxiv [Preprint]* 2021. doi:10.1101/2021.08.16.21262044.
- [16] Machado RRG, Glaser T, Araujo DB, Petiz LL, Oliveira DBL, Durigon GS, *et al*. Inhibition of Severe Acute Respiratory Syndrome Coronavirus 2 Replication by Hypertonic Saline Solution in Lung and Kidney Epithelial Cells. *ACS Pharmacol Transl Sci* 2021;4(5):1514–1527. doi:10.1021/acspstci.1c00080, PMID:34651104.
- [17] Drug Approval Package Trasylol (Aprotinin) Injection (Updated August 28, 1998) Available from: [https://www.accessdata.fda.gov/drugsatfda\\_docs/nda/98/020304s004.cfm](https://www.accessdata.fda.gov/drugsatfda_docs/nda/98/020304s004.cfm). Accessed June 10, 2022.
- [18] Zhirnov OP, Klenk HD, Wright PF. Aprotinin and similar protease inhibitors as drugs against influenza. *Antiviral Res* 2011;92(1):27–36. doi:10.1016/j.antiviral.2011.07.014, PMID:21802447.
- [19] Bojkova D, Bechtel M, McLaughlin KM, McCreig JE, Klann K, Bellinghausen C, *et al*. Aprotinin Inhibits SARS-CoV-2 Replication. *Cells* 2020;9(11):E2377. doi:10.3390/cells9112377, PMID:33143316.
- [20] Liu Y, Liu J, Johnson BA, Xia H, Ku Z, Schindewolf C, *et al*. Delta spike P681R mutation enhances SARS-CoV-2 fitness over Alpha variant. *Cell Rep* 2022;39(7):110829. doi:10.1016/j.celrep.2022.110829, PMID:35550680.
- [21] Zhang J, Cai Y, Xiao T, Lu J, Peng H, Sterling SM, *et al*. Structural impact on SARS-CoV-2 spike protein by D614G substitution. *Science* 2021;372(6541):525–530. doi:10.1126/science.abf2303, PMID:33727252.
- [22] Zhang J, Cai Y, Lavine CL, Peng H, Zhu H, Anand K, *et al*. Structural and functional impact by SARS-CoV-2 Omicron spike mutations. *Cell Rep* 2022;39(4):110729. doi:10.1016/j.celrep.2022.110729, PMID:35452593.
- [23] Ziegler CGK, Miao VN, Owings AH, Navia AW, Tang Y, Bromley JD, *et al*. Impaired local intrinsic immunity to SARS-CoV-2 infection in severe COVID-19. *Cell* 2021;184(18):4713–4733.e22. doi:10.1016/j.cell.2021.07.023, PMID:34352228.
- [24] Ahn JH, Kim J, Hong SP, Choi SY, Yang MJ, Ju YS, *et al*. Nasal ciliated cells are primary targets for SARS-CoV-2 replication in the early stage of COVID-19. *J Clin Invest* 2021;131(13):148517. doi:10.1172/JCI148517, PMID:34003804.
- [25] Böttcher-Friebertshäuser E, Klenk HD, Garten W. Activation of influenza viruses by proteases from host cells and bacteria in the human airway epithelium. *Pathog Dis* 2013;69(2):87–100. doi:10.1111/2049-632X.12053, PMID:23821437.